Paper No. 63

MATHEMATICAL MODEL OF MOLECULAR FLOW IN THE NASA-JSC THERMAL-VACUUM CHAMBER A

A. L. Lee and S. J. Robertson, *Lockheed Missiles and Space Co., Huntsville, Alabama;* Horst K. F. Ehlers, *NASA-Johnson Space Center, Houston, Texas*

ABSTRACT

A new computer program has been developed for the math modeling of molecular flux inside a typical large thermal-vacuum chamber. It can be applied in four general areas: prediction, evaluation and improvement of the chamber performance; prediction of contamination migration; location of sources of leaks and outgassing; and design of new thermal-vacuum chambers.

INTRODUCTION

Thermal-vacuum chambers of various capacities installed at National Aeronautics and Space Administration (NASA) centers are extensively used for space simulation testing. One of the major concerns of such testing is the maintaining of required environmental conditions, specifically the preventing of the contamination of the most sensitive test article components with undesirable molecules released by materials such as outgassing paints, vacuum pump oils, etc. The ability to identify and locate in-chamber gas leaks and sources of contamination is of prime importance so that they may be controlled or removed. Current practices in fulfilling this need at NASA-Johnson Space Center's (JSC) thermal-vacuum chamber A involve the use of directional molecular flow sensors, referred to as the Directional Gas Flow Measurement (DGFM) system[1]. The accuracy of the DGFM system has been restricted when gas or contamination sources are located behind the liquid nitrogen (LN_2) cooled shroud, below the chamber floor, or when other chamber structures are located between source and sensor. In addition, the sensor cannot always be positioned at locations where the need for molecular flux measurements is greatest (e.g., near the spacecraft).

There appears to be a need for some theoretical model that relates molecular flux rates and gas or

contamination sources in order to solve these and other problems that are normally encountered in thermal-vacuum testing; and, as a result, help reduce the cost in the perfcrmance of these tests. A truly analytical model exists sc far only fcr space environment simulaticn chambers and test articles of ideal spherical symmetry and concentric arrangement. This model usually helps in making gross estimates of molecular flow rates in most chambers; it does not provide sufficiently accurate data to meet the actual requirements rising from practical thermal-vacuum testing. This is true even for chambers of "spherical" design.

Mathematical modeling based on more realistic chamber and test article configuration appears to allow reasonable and adequate prediction and extrapolation of molecular flux during testing.

A new Monte Carlo computer program was developed for the mathematical simulation of molecular flux inside a typical thermal-vacuum chamber, such as chamber A at NASA-JSC. This prcgram constitutes a new approach in developing a tool that may be used to accomplish any of the following tasks:

1. Assisting in interpreting the readings of a molecular flux sensor in order to locate and identify gas leaks and contamination sources.
2. Predicting the molecular flow rates in specific locations depending on test configuration (contaminent migration).
3. Predicting and evaluating the adequacy of space vacuum simulation and test envircnment condition, specifically with respect to level of contamination.
4. Predicting the effect of abnormal test article and chamber conditions (aid in troubleshooting).
5. Predicting and evaluating the effects of chamber modifications and configuration on test objectives. (test planning)
6. Aiding in the design of new vacuum chambers.

The program therefcre permits the study and evaluation of specific test configurations before any hardware is produced thereby eliminating possible costly configuration changes after hardware is manufactured.

This paper describes characteristic features of the mathematical model developed by Lockheed Missiles & Space Company, Inc., (LMSC) on contract to NASA-JSC and some specific application cases.

MATHEMATICAL MODEL

The mathematical approach taken in developing the molecular flow model involves variations of the Monte Carlo method. During the course of the model development, it became apparent that a complete modeling of the entire chamber geometry, using the classical Monte Carlo technique, would require an unreasonable amount of computer time and, in some cases, would be unproductive. The reasons for this will be made clear in the following discussion. The approach taken, therefore, was directed toward developing a model which would provide the optimum combination of utility and computer usage economy.

Consider the schematic of the chamber A geometry shown in figure 1. The leak detector sensors have been located within the main chamber area near the interior surface of the LN_2 shroud. Molecular flow originating from a source located within the main chamber will reach the sensors by direct flight, providing there are no intervening obstacles, and by indirect flight after undergoing collisions with the chamber interior surfaces and other molecules. Molecular flow originating behind the LN_2 shroud will undergo a large number of collisions behind the shroud before eventually escaping into the main chamber area through one of the gaps or openings in the shroud. Finally, molecular flow originating within the lower dome area, and particularly within the plenum chamber, will undergo an enormous number of collisions before eventually migrating into the main chamber. In fact, it can be shown that the flow in the plenum chamber becomes randomized to the point that the location of the source becomes irrelevant to the molecular flow distribution. This means that it would be impossible to determine the source location by measuring molecular flow characteristics at a point outside of the plenum chamber.

The nature of the Monte Carlo method is such that each collision that each molecule undergoes represents calculations that have to be made and, hence, computer time usage. With the large number of sample molecules that must be generated to achieve statistical accuracy, a prodigious amount of computer time can be required for a single run.

One of the primary purposes of the mathematical model is to calculate the molecular flow rate at the DGFM sensor location. To accomplish this by the classical Monte Carlo method, the geometry of the sensor must be modeled, and the number of sample molecules that eventually enter the sensor are counted. Since the sensor diameter is of the order of an inch while

the chamber diameter is of the order of 60 feet, the probability of a single sample molecule entering the sensor is, for all practical purposes, infinitesimal. The number of sample molecules required for a molecular flow rate calculation, therefore, would approach infinity. A compromise can be made by utilizing a larger diameter sensor in the mathematical model. This would, in effect, average the calculated flow rate over a larger area and would still require a large sample size to achieve statistical accuracy. The method finally selected eliminates the need for large sensor diameters and actually calculates the flow rate at a point using a combination of Monte Carlo and view factor concepts. Compared to the classical Monte Carlo technique, this method is extremely economical from a computer usage standpoint and, in most cases, is a great deal more accurate. This method is designated the ray tracing technique and is described in the following paragraphs.

Ray Tracing Technique

The ray tracing technique is based on the fact that for molecules traveling directly from a source to a point, the molecular flux can be calculated directly from a simple view factor relationship without a need for counting sample molecules. This concept is extended to include scattering from other molecules and from walls by utilizing certain Monte Carlo principles. Consider the hypothetical molecular flow configuration shown in figure 2. The molecular flux, q_1, at the sensor location, due to molecules streaming directly from the source, is given by the following equation:

$$q_1 = \frac{\dot{m}_o \cos\alpha_1 \cos\gamma_1}{\pi r_{a-c}^2} \exp(-r_{a-c}/\lambda) \qquad (1)$$

where $\dot{m}_o$ is the source strength, r_{a-c} is the distance between source and sensor, λ is the mean free path, and α_1 and γ_1 are given in figure 2. The source is assumed to emit in a cosine law distribution. The exponential factor accounts for attenuation due to intermolecular collisions.

For molecules arriving indirectly at the sensor location after undergoing collisions, a variation of the Monte Carlo technique is used. First, a representative sample of molecular trajectories is selected randomly according to a cosine distribution, and each

of these trajectories is traced to a point of intersection with a wall. Each of these sample trajectories is considered to represent a flow rate of $\dot{m}_o / N$, where N is the number of trajectories in the sample. For each of these trajectories, an amount $(\dot{m}_o / N)[1 - \exp(-r_{a-b} / \lambda)]$ will be scattered from the beam by intermolecular collisions. The remaining $(\dot{m}_o / N) \exp(-r_{a-b} / \lambda)$ will reach the point of intersection with the wall where a fraction C, the capture coefficient, will remain stuck to the wall. The remaining fraction $(1-C)$ will be scattered in a cosine distribution. Those molecules attenuated from the beam by intermolecular collisions are represented by a new source of strength $(\dot{m}_o / N_o)[1 - \exp(-r_{a-b} / \lambda)]$ located at a point on the trajectory at a distance from the original source. If $\lambda > r_{a-b}$, these scattered molecules are neglected. This new source emits in a cosine distribution in the direction of the trajectory. The molecules that reach the point of intersection with the wall are represented by a new source of strength $(1 - C)(\dot{m}_o / N_o)\exp(-r_{a-b} / \lambda)$ at the point of intersection, again with a cosine distribution. These new sources will contribute to the flux at the sensor location according to

$$q_2 = (1-C)\frac{\dot{m}_o}{N_o}\exp(-r_{a-b}/\lambda)\frac{\cos\beta\cos\gamma_2}{\pi r_{b-c}^2}\exp(-r_{b-c}/\lambda) + \frac{\dot{m}_o}{N_o}\left[1-\exp(-r_{a-b}/\lambda)\right]\frac{\cos\delta\cos\gamma_3}{\pi r_{d-c}^2}\exp(-r_{d-c}/\lambda) \quad (2)$$

This procedure may be repeated as many times as accuracy requires or economy permits, so that the total flux q at the sensor location is given by

$$q = q_1 + \sum_{i=1}^{N_o} q_{2_i} + \sum_{i=1}^{N_o}\sum_{j=1}^{N_o} q_{3_{ij}} + \cdots\cdots \quad (3)$$

In practice, it is unnecessary to go beyond the second wall collision (q_3), since additional collisions merely serve to randomize the molecular flow into the background pressure. The results presented in a later section were obtained using values of N_o around 250 for the first collision and values of N_1 around 25 for the second collision. This represents a considerable

gain in economy over the classical Monte Carlo approach, which usually requires a sample size of from 10,000 to 100,000 to achieve even moderate accuracy. In addition to the gain in economy, the statistical fluctuations associated with Monte Carlo calculations are practically eliminated.

Modeling of Sensor

Another gain in economy is achieved by computing a directional distribution of molecular flux at the sensor location. From this directional distribution, the molecular flux can be determined for any direction that the sensor might be oriented. This allows a single computer run to develop data which would otherwise have required several runs. In the results presented in a later section, a single run simulates both horizontal and vertical scans of the DGFM sensors.

The directional distribution is obtained by dividing the vertical and horizontal angles (latitudinal and longitudinal) into increments, and each contribution, q_{ij}, to molecular flow at the sensor location is determined to correspond to one of these increments, where i and j refer to vertical and horizontal angle increments. The molecular flux, q_{lm}, corresponding to a particular sensor direction is then obtained from

$$q_{l,m} = \sum_{ij} q'_{ij} \cos\theta_{ij;lm} \qquad (4)$$

where $\theta_{ij;lm}$ is the angle between the sensor direction and the increment ij, and the summation is made over angular increments within the field of view of the sensor.

Classical Monte Carlo

In a previous section it was pointed out that molecular flow originating in the lower dome region would undergo a large number of collisions before eventually migrating into the main chamber area where it could be detected by the DGFM sensors. For this reason it was decided to treat this region separately from the main chamber. Because of the large number of wall collisions, and the fact that a sensor simulation was not required, the classical Monte Carlo approach was used to calculate molecular flow characteristics in this region. In this approach, a representative sample of molecular trajectories is selected randomly from a cosine distribution at the source location, and

each trajectory is traced until it leaves the system. The molecular flux at some point of interest, such as the diffuser grid between the lower dome and main chamber, can be calculated by counting the number of molecules that intersect a unit area of surface.

Chamber Geometry Simulation

The overall chamber geometry was simulated in separate sections, primarily depending on the mathematical approach being utilized.

Main Chamber: The main chamber, including helium panels, LN_2 shroud, LN_2 panel, test article and sensors, was included in one program with molecular flow being treated using the ray-tracing technique. The geometry simulated in this program is shown in figure 3. The dimensions of the chamber and the locations of the source and sensor were made arbitrary. The program can handle one source and 2 sensor locations during one run. The test article geometry is arbitrary to the extent that it can be constructed of combinations of cylinders, spheres, cones, disks and plane quadrilaterals. The locations and dimensions of these subshapes are made arbitrary to allow the simulation of complex test article geometry.

Plenum Chamber: Flow in the plenum chamber was calculated using the classical Monte Carlo technique with the geometry simulated as shown in figure 4. The program calculates the flow from a source and records the distribution of collisions around the chamber wall. This program was developed primarily to demonstrate the fact that the large number of wall collisions effectively randomizes the flow into a background pressure and to calculate the flow of migrating contamination in and out of the plenum chamber.

Repressurization Plenum: Flow in the repressurization plenum was modeled by the classical Monte Carlo technique using the geometry in figures 4 and 5. The repressurization diffuser duct was not included because the time and effort required to model the complex geometry did not appear to be justified by the impact of the duct's presence on the molecular flow distribution. Test calculations made without the duct indicate that, except for sources located inside the duct, the flow tends to become randomized to a large extent on all sides of the duct, so that the duct's influence on the flow is essentially nullified.

The computer program is set up to first compute the transmission probability for flow through the channel formed by the trays under the main chamber floor, and then through the diffuser grid. After this

522-137 O - 73 - 50

transmission probability is computed, the molecular flux along the diffuser grid surface is calculated as a function of angular position around the chamber. The results of this computation can be used as inputs to the main chamber program.

Solar Simulators: In the main chamber program, the solar simulators are treated as solid plates without gaps. The reason for this is that the gaps are considered to be negligibly small compared to the principal openings in the LN_2 shroud. A separate program, based on the classical Monte Carlo technique, was developed to simulate molecular flow from a source behind the solar simulator. The individual lamps are represented as circular disks set off from the wall on the same plane. The diameter of the circles are made arbitrary and allowed to overlap to simulate varying gap sizes.

Diffusion Pump Ports: A separate program, based on the classical Monte Carlo technique, was developed to trace the backstream flow from the diffusion pump ports as well as the molecules that were pumped by diffusion pumps. The pump ports are located behind the LN_2 shroud. In order to trace the molecular flow between the LN_2 shroud and the chamber wall, additional structural features and cooling surfaces have to be considered. These include the cylindrical shield at the door, LN_2 cooled baffles over each manlock and LN_2 cooled surfaces on and around manlocks and around the side sun simulator. The result of this program tabulates the quantities of the molecules which are deposited on certain surfaces, pumped by diffusion pumps, and which escape into the test area.

APPLICATIONS

The math model can be applied in three general areas: evaluation and improvement of the chamber performance; prediction of contaminant migration; and, location of sources of leaks and outgassing.

The performance of a thermal-vacuum chamber can be rated by its selfcontamination factor, Z, which is defined as the ratio of the number of molecules returning to the test vehicle surface to the number of molecules leaving the vehicle surface. A low value for Z represents a good space simulation. The Z factor depends primarily on the capture coefficients of chamber surfaces and the relative values of the test vehicle and the thermal-vacuum chamber. However, the location of cold surfaces and the direction of outgas flux affect the value of Z also. The Z factor and the average capture coefficient of the chamber are calculated at the same time. Capture coeffi-

cient, C_{av}, is defined as the fraction of molecules being captured by the cooled wall at its first encounter. C_{av}, like Z, is also dependent on local capture coefficients, location of cold surfaces and direction of flow.

Table 1 shows the results of a simulation using the Apollo command and service module (2TV-1) as the test vehicle. C1 and C2 are the capture coefficients for the LN_2-cooled and He-cooled panels, respectively.

TABLE I

Case	C1	C2	Z	C_{av}
1	0.00	0.01	0.668	0.026
2	0.85	0.97	0.016	0.848
3	0.20	0.95	0.118	0.362
4	0.20	0.95	0.168	0.304
5	0.10	0.90	0.166	0.250
6	0.10	0.90	0.142	0.396
7	0.10	0.90	0.112	0.408
8	0.10	0.90	0.150	0.224
9	0.10	0.90	0.138	0.246
10	0.10	0.90	0.1418	0.3048

Cases 1 through 4 simulates the uniform outgassing of the test vehicle by putting a uniformly emitting point source at the center of the vehicle geometry. Cases 1 and 2 compare very favorably with previously calculated results (Ehlers, 1970)[2], where Z was 0.70 and 0.003 for zero pumping and LN_2 coldwall pumping, respectively. Cases 3 and 4 are under identical conditions except that in case 4 half of the He panels are shut off. Each of the "off" panels alternate with "on" panels. Note the corresponding increase in Z and reduced C_{av} value. Cases 5 through 8 simulate the conditions in which gas is released on the side of the rotating vehicle at 90 degree intervals. When the source is facing the large door or the side sun cutout, the local average capture coefficient is markedly reduced due to the reduced area covered by the He panel. This effect is clearly shown in the increased values of Z in cases 5 and 8. Case 9 simulates the outgassing for a point located on the command module surface. Case 10 is the accumulated average for cases 5 through 9.

The movement of contaminants can be traced either from one partition of the chamber to another or from the source to the surfaces within the same partition.

Table 2 tabulates the results of contaminant backstreaming from diffusion pump ports on the same level. CPP is the diffusion pump port capture probability.

The coordinates of sources are normalized by the chamber radius. Equivalent capture coefficients for noncondensible gases due to pumping at the diffusion pump ports can also be calculated for the cutouts on the LN_2 shroud. The simulation is made by treating the LN_2 shroud cutout as an area source, and counting the fraction of molecules pumped by the diffusion pumps. A calculation shows that the equivalent capture coefficients for manlock cutouts 1, 2, and 3 are 0.013, 0.04, and 0.0956, respectively.

In order to calculate the migration of gas molecules from one subchamber to another, the conductivity is calculated for the passage between the repressurization plenum and main chamber. The result is plotted versus the capture coefficient of the repressurization diffuser in figure 6. An example of the molecular distribution over the repressurization diffuser when a source is located beneath is shown in figure 7. This distribution can be detected by the sensors in the chamber.

When a leak or contamination source is to be located, the position of the sensor itself is very important. When the source is in the field of view of the sensor, there is an unambiguous peak in the direction of the source. When the source is obscure, either behind the test vehicle or behind the LN_2 panels, the reading would show more than one peak which may depict the shadow of the vehicle or the cutouts on the panel. A source was placed at a DP port (-.809,.588,1.29) for example. Two sensors were placed behind LN_2 shroud, and two were inside the shroud. The locations of sensors and source and relevant features of the chamber are shown in figure 8. The simulated reading of sensor ① showed a strong flux from side sun cutout. The horizontal reading is shown in figure 9. Sensor ② readings were generally lower in magnitude. The peak pointed to the direction of manlocks. Interpreting the readings of sensors ① and ② it is logical to conclude that a source was behind the LN_2 shroud at the location probably closer to side sun cutout than to manlock cutouts. The sensors ③ and ④ behind the LN_2 shroud showed peaks pointing directly to the source location.

TABLE 2

Location of Source	(-.951,-.309,1.29)	(-1.0,0,1.29)	(-.951,.309,1.29)	(-.809,.588,1.29)
Total Condensed (%)	92.0	92.6	92.2	90.8
Due to C1	0.6	0.4	0.6	1.0
Due to C2	91.4	92.2	91.6	89.8
On Manlcck Dr. 1	0.2	0.0	0.2	0.0
Cn Manlcck Dr. 2	2.0	1.4	0.6	0.0
On Manlcck Dr. 3	0.8	0.4	0.0	0.0
On Side Sun Cooled Area	0.0	0.0	1.4	3.0
Cn Conic Top	0.8	1.4	1.0	1.0
On Baffle Over Manlock 1	0.0	0.2	0.2	0.2
On Baffle Cver Manlock 2	0.8	0.4	0.4	0.2
On Baffle Over Manlock 3	0.4	0.2	0.2	0.0
Escaped Through Side Sun Cutcut	0.4	0.8	2.0	4.8
Flccr Grid	0.0	0.0	0.2	0.2
Manlock 1	0.0	0.0	0.0	0.0
Manlock 2	4.4	0.4	0.4	0.0
Manlock 3	0.0	0.2	0.0	0.0
Pumped by Diffusion Pump	3.2	6.0	5.0	4.2

C1 = 0.01, C2 = 0.50, CPP = 0.95

CONCLUSIONS

The mathematical model is a powerful tool in the design, improvement and day-to-day operation of a thermal-vacuum chamber. Simulations of new configurations can easily be run with the model before costly hardware is manufactured.

The effectiveness of the space simulation can be determined by its Z factor. The values of Z and the average capture coefficient, hence the overall pumping speed, can be improved by relocating the He panels and the diffusion pumps used, adding more pumping capability, shielding hot spots, etc. Because of the numerous parameters involved, the mathematical model is the most logical way to determine the optimum configuration. On the other hand, adverse effects can be predicted when new surfaces, such as IR heaters, are introduced into the chamber.

Contamination has always been a matter of concern in thermal-vacuum testing. The main concern is the migration path and distribution at specific locations. If the movement of contaminating molecules can be traced, it might be possible to control the contaminant flow. The model would provide a useful tool in this respect.

The usefulness of the model is very broad, limited only by the user's imagination. The model is programed specifically for the NASA-JSC chamber A. The geometric flexibility inherent in the model, however, allows its use in a variety of chambers.

REFERENCE

1. Ehlers, H. K. F., "Directional Molecular Flow Analysis and Leak Detection With a Rotatable Gas Analyzer in a Large Space Simulation Chamber," NASA SP-298, pp 789-795.

2. Ehlers, H. K. F., "Pressure Measurements and Gas-Flow Analysis in Chambers A and B During Thermal-Vacuum Tests of Spacecraft 2TV-1 and LTA-8," J. Spacecraft and Rockets, Vol. 7, No. 4, April 1970.

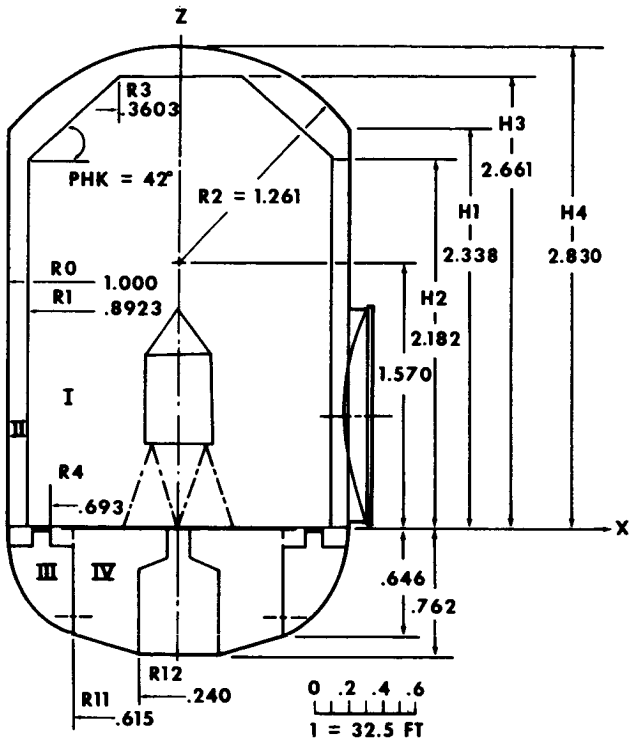

Fig. 1 - Schematic of Chamber "A" model

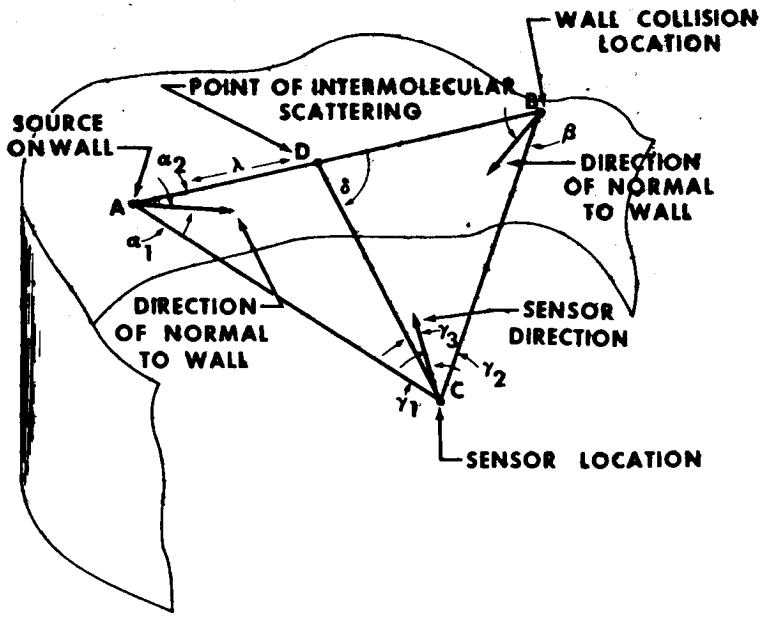

Fig. 2 - Illustration of ray-tracing technique

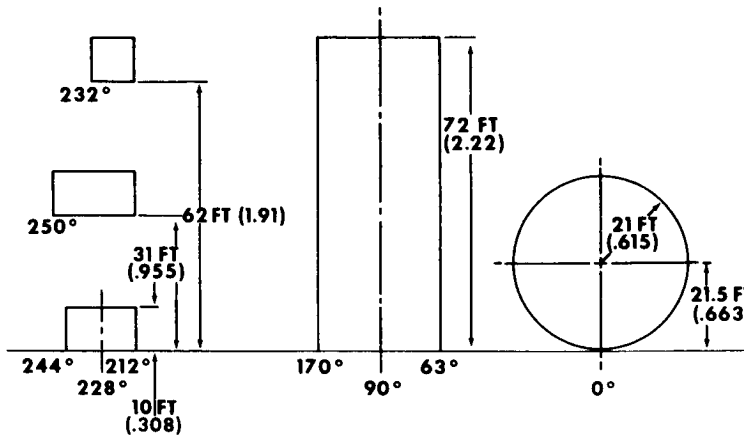

Fig. 3 - Developed view of LN_2 shroud openings (R1 = 29') (normalized quantities in parentheses)

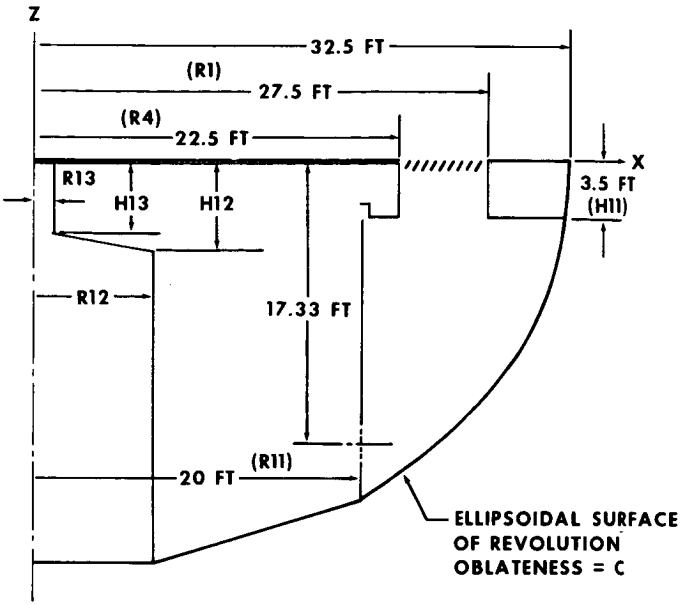

Fig. 4 - Geometry of repressurization plenum

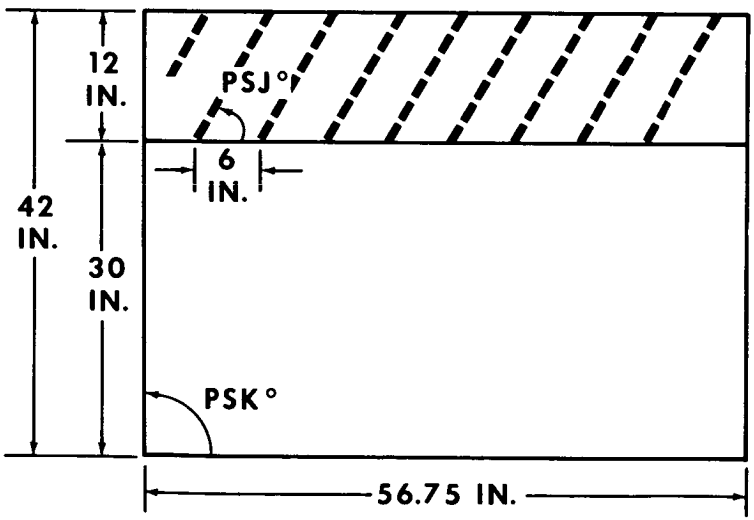

Fig. 5 - Model of passage from repressurization plenum to main test area

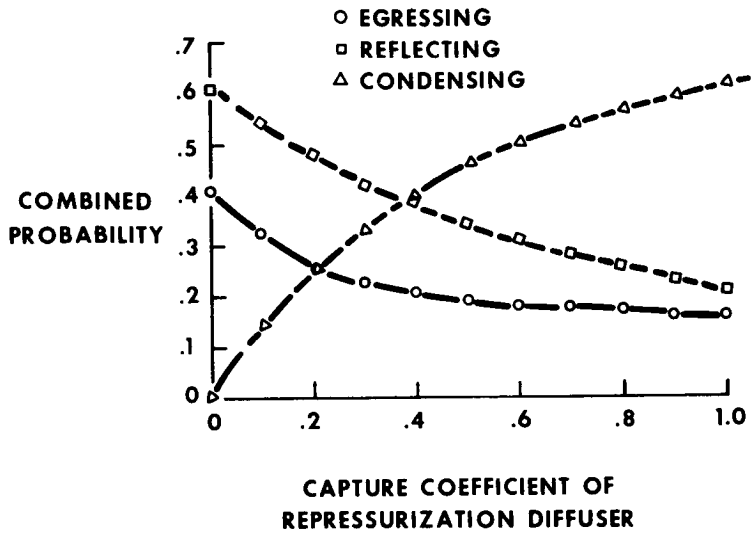

Fig. 6 - Probabilities of transmission, reflection and adsorption of the passage between repressurization plenum and main chamber

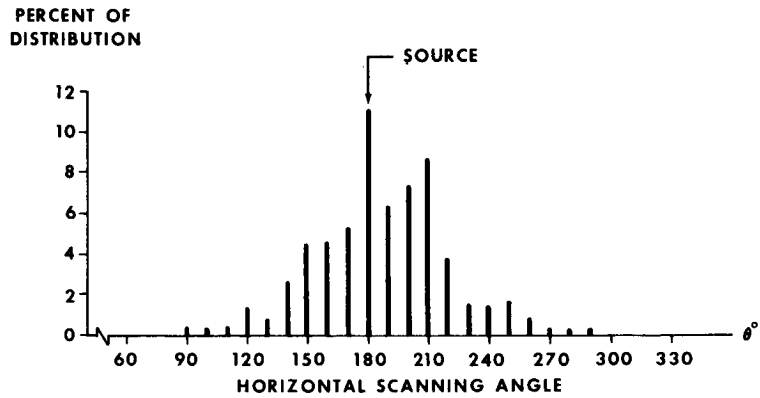

Fig. 7 - Molecular distribution over repressurization diffuser with a source underneath at θ = 180 degrees

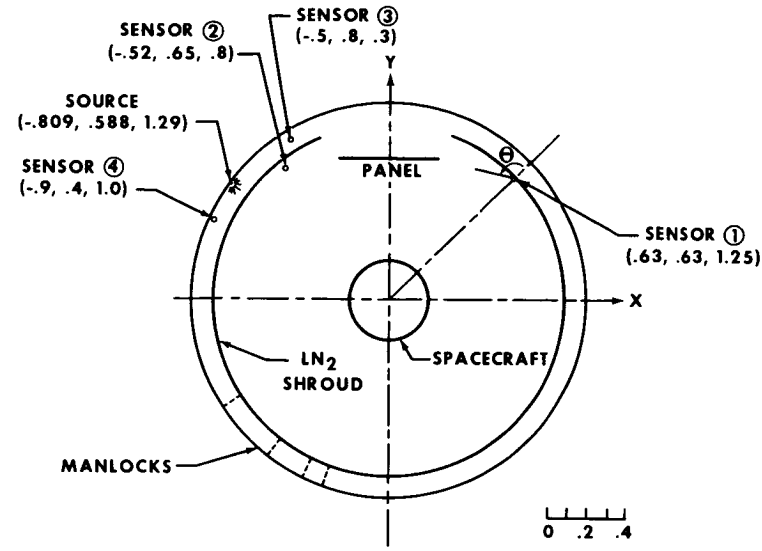

Fig. 8 - Schematic of chamber layout

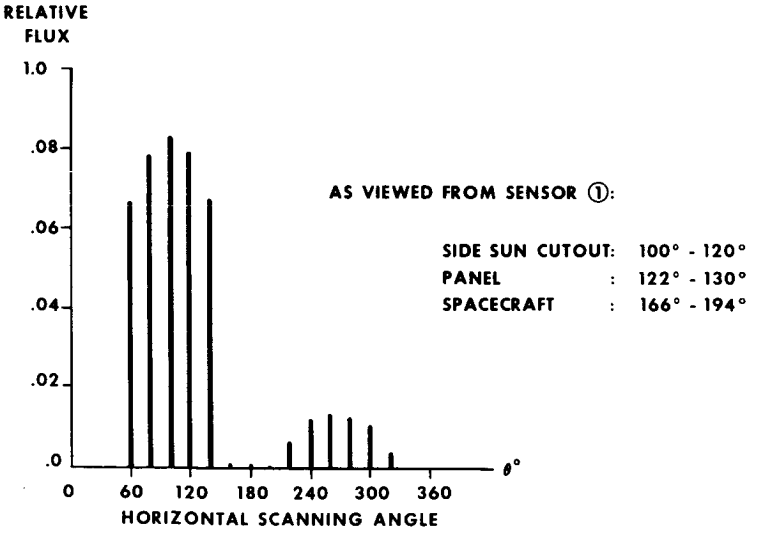

Fig. 9 - Horizontal scanning of sensor ① over source at (-.809, .588, 1.29)